Dynamical Characterization of the Loop Current Attractor

G. Liu[1], F. Falasca[1,2] and A. Bracco[1*]

1 School of Earth and Atmospheric Sciences, Georgia Institute of Technology, Atlanta, GA, USA

2 Courant Institute of Mathematical Sciences, New York University, New York, NY, USA

Corresponding author: Annalisa Bracco (abracco@gatech.edu)

Key Points:

- A metric from dynamical system theory is applied to the Gulf of Mexico to characterize the attractor of the Loop Current.
- Model products (reanalysis and hindcast) portrait a different local dimension than GCOOS data.
- Results point to where improvement is needed for better ocean forecast skills.
-

Abstract

The Gulf of Mexico circulation is modulated by a mesoscale current, the Loop Current (LC), and large anticyclonic eddies that detach from it. The LC dynamics are recurrent, and its evolution is in and from a few preferential states. This observation points to the existence of a low-dimensional dynamical attractor. Building upon advancements in dynamical system theory, this work characterizes the average and instantaneous dimensions of such an attractor. The instantaneous dimension and its evolution in time are compared among an altimeter-based dataset, an ocean reanalysis and an operational hindcast. The LC complexity, measured by its dimension, differs among them, especially when the dimension is high. During shedding events, on the other hand, differences between datasets emerge in the second principal component. The information provided by this analysis is relevant to operational ocean forecasts and points to where improvement should occur.

Plain Language Summary

We characterize the evolution of the large-scale circulation of the Gulf of Mexico, which is dominated by the Loop Current, using a metric from dynamical system theory. Comparing results from an altimetry-based sea surface height dataset and model-based products, it is found that the model misrepresents in part the set of states toward which a system tends to evolve. This is the case especially when the Loop Current is in an intermediate configuration, not fully retracted towards Cuba or extended towards the Florida Panhandle. This analysis points to aspects that models should improve before ocean forecasts for the region can be extended successfully beyond five days. The forecast extension, which

is theoretically supported by our work, would bring societal benefits to people working in the oil and fishery industry and those living on the coastlines of a basin often traversed by tropical storms and hurricanes.

1 Introduction

The circulation of the Gulf of Mexico is dominated by the anticyclonic Loop Current (LC). The LC enters the Gulf from the Yucatan Channel and exits it through the Florida Straits, bringing into the enclosed basin between 23 and 27 Sv (1 Sv = 10^6 m^3s^{-1}) of relatively warmer, saltier and nutrient poor waters (Johns et al., 2002). The LC is the largest mesoscale feature in the region, about 200 - 300 km wide and 1200 m deep, with surface velocities of 0.8 ms^{-1} increasing to 1.5 ms^{-1} below the mixed layer (Gordon, 1967).

The LC's position varies greatly over time. It can be found in its retracted state in the Yucatan Channel or in its extended state all the way into the De Soto Canyon, and any state in between. At irregular intervals, the LC in its extended state sheds a Loop Current eddy (LCE) or Ring, with size of 200 km in diameter. The large anticyclone then migrates slowly westward (Hamilton, 1990; Lipphardt et al., 2008), losing coherence once it reaches the continental shelf on the western boundary. The time interval at which the LCEs form varies between half month to over a year, with limited evidence of preferred shedding events in spring and fall (Hall and Leben, 2016).

The evolution of LC and LCEs in the Gulf is generally accompanied by the formation of smaller mesoscale eddies, cyclonic and anticyclonic (e.g. Gopalakrishnan et al., 2013). LC and LCEs, together with the smaller eddies, are often called the LC system, or LCS. The mechanisms and processes that control the penetration of the LC into the Gulf of Mexico and trigger the Rings' separation are neither well simulated and forecasted by ocean models, nor fully understood (National Academies of Sciences and Medicine, 2018). More skillful predictions of the LC dynamics would have consequential societal benefits, ranging from improved weather forecasts, especially relevant in the event of tropical storms and hurricanes, to better oil spill and emergency preparedness and response, and improved fishery management.

Recent theoretical advances (McMahon et al., 2021) found in an idealized 1-layer model that the LC-like system transitions between five steady states, three stable and two unstable. The analysis suggests that relatively few degrees of freedom may be sufficient to describe the LC system most of the time, and its potential predictability may be higher than previously realized and currently achieved by ocean forecast systems. In this work, we aim to characterize and compare the attractor of the LC in an observational dataset, a reanalysis and a model analysis of the Gulf of Mexico, adopting a metric from dynamical system theory.

Oceanic motions are chaotic. In an enclosed system, these motions are typically contained on low-dimensional attractors (Lorenz, 1980) with an average dimension that quantifies the number of degrees of freedom needed to describe

the flow (for the well-studied double-gyre case see e.g. Primeau, 1998 and for a general introduction to dynamical system approaches to physical oceanography Dijkstra, 2000). While the average dimension of the LC system - or of any chaotic system - is an important, first-order, property that should be correctly reproduced by models, its transient states are also of interest for forecasting purposes. The dynamical properties of these LC states, from retracted to extended, depend on the instantaneous, instead of the average, dimension of the attractor (Vautard and Ghil, 1989). Lucarini et al. (2016) have shown that these instantaneous properties can be uniquely identified by their *local dimension*, which has been so far applied to atmospheric fields (Faranda et al., 2016; Hochman et al., 2019; De Luca et al., 2020; Messori et al., 2021; Falasca and Bracco, 2021). In the case of the LC system the comparison between this metric calculated on the observational and modeled datasets points to important limitations of the model realizations and suggests ways to improve the forecast skill.

2 Methods and Data

The high-dimensional dynamics of dissipative flows such as the ocean typically live on nonlinear, low-dimensional "inertial manifolds" or attractors (Foias et al., 1988; Gudorf, 2021). Here we characterize the Loop Current (LC) attractor using the instantaneous (*local*) dimension metric proposed in Lucarini et al. (2016).

The instantaneous dimension indicates the number of degrees of freedom (DoF) of each state of the attractor and describes, in physical space, the largest, dominant mesoscale features, which are given by the LC in the eastern half of the Gulf of Mexico and the Rings in the western one. While very useful to establish the predictability potential of a given dynamical system, $d(\ )$ has been applied only to a handful of flows so far because a robust way of calculating it has been proposed only recently and its computation requires relatively long, spatially extended high-frequency measurements. The methodology stems from theoretical advances in understanding Poincaré recurrences in chaotic systems and their connection to extreme value theory (Lucarini et al., 2016). The instantaneous dimension relates to the density of state space points in a neighborhood of the state (i.e. how many similar configurations can be found) and quantifies the number of directions the system can evolve from/into. If the number of states considered is sufficiently large, an estimation of the attractor dimension can be obtained from the average over time of the local dimensions as $D = < d(\ ) >$. Faranda et al. (2016) verified that this is indeed the case for the Lorenz system.

In more detail, let us consider a trajectory of a geophysical flow as a high-dimensional vector X $R^{N,T}$, with N being the dimensionality of the spatial grid and T the number of time steps. Given a state = X(t) at time t, we define our observable as:

g(X(t),) = -log((X(t),)) , (1)

where g(X(t),) represents the distance between a state and other states on the trajectory, (x, y) is the Euclidean distance between two vectors x and y

and the logarithm discriminates between close recurrences. The minus sign turns minima into maxima and is chosen for practical convenience.

Freitas et al. (2010) and Lucarini et al. (2016) proved that the probability that the flow returns in the neighbourhood of a state converges to a Generalized Pareto Distribution:

$$P(g(X(t),) > s(q,)) \quad \exp(-\frac{u( )}{( )}) \ . \ (2)$$

Here is the scale parameter of the Pareto distribution and *s(q,)* is a threshold defined as the *q*th quantile of each time series g(X(t),) with q = 0.96. Exceedances of g(X(t),) over *s(q,)* are referred to as *u*( ) and represent recurrences of the state .

Lucarini et al. (2016) proved that the *instantaneous* or *local dimension* of a state , which yields the number of degree of freedom, can be computed as the inverse of ( ), i.e. $d( ) = 1/ ( )$.

Robust estimates of d require high frequency, spatially well resolved data, covering a sufficiently long period so that recurrences can be captured. We chose SSHa (sea surface height anomalies) as a representative field for the large-scale mesoscale circulation in the Gulf of Mexico and adopted the GCOOS (Gulf of Mexico Coastal Ocean Observing System) SSHa dataset, in which observations from four altimetry satellites are merged into daily gridded maps following Leben et al. (2002). GCOOS SSHa data have a spatial resolution of 0.25 ° × 0.25° and we consider the available period January 2004 - December 2019. To date, satellite observations are the best available long-term oceanographic data available in the GoM, despite their limited spatial and temporal resolution. The geostrophic currents derived from GCOOS have been shown to be somewhat more accurate than those from data assimilative models to hindcast drifter trajectories observed in the eastern Gulf of Mexico during spring and summer 2010 (Liu et al., 2014). Here the GCOOS dataset is compared to the SSHa field from the HYCOM-NCODA reanalysis for the Gulf of Mexico available with 3-hourly frequency on a 0.04° × 0.04° horizontal resolution grid. The reanalysis is produced by the Naval Oceanographic Office that provides also a real-time, widely used forecast for the basin. The reanalysis system assimilates satellite altimeter and SST observations as well as all available in-situ temperature and salinity profiles using the Navy Coupled Ocean Data Assimilation (NCODA) system (Cummings and Smedstad, 2013). Following repeated upgrades in the forecasting system, only limited periods have been run for any given version of the HYCOM-NCODA reanalysis. We consider one of the longest experiments available at the resolution mentioned, GOMu0.04/Exp50.1, covering the GCOOS data range until 12/31/2012. The ocean model is forced by fields from the National Centers for Environmental Prediction (NCEP) Climate Forecast System Reanalysis (CFSR, Saha et al., 2010), and the boundary conditions are from the global HYCOM reanalysis. Additionally, we consider the GOMl0.04/expt_31.0 and the GOMl0.04/expt_32.5 analysis or hindcast, available respectively from April 2009 to July 2014 and from April 2014 to February 2019 at the same hori-

zontal resolution of the reanalysis to extend GOMu0.04/Exp50.1 from January 2013 (GOMl0.04/expt_32.5 is used over the common period April-June 2014). The analysis is run in real time, assimilates SST and profiles using FGAT (first guess at appropriate time) and is forced by atmospheric fields from the Center for Ocean-Atmospheric Prediction Studies (COAPS), using different and better resolved wind and heat forcing compared to the reanalysis. In this case HYCOM is used to perform one day of analysis using all observations received since the previous analysis. The analysis data are made available within two days after the integration.

Qualitative assessments of current products derived from altimetry data and assimilative numerical models, were performed in the eastern Gulf of Mexico -the region of interest in our work- using satellite-tracked drifter trajectory observations (Liu et al., 2014), as mentioned. Altimetry-derived products (SSH and geostrophic currents) have been shown to be accurate as - and at times more than - data-assimilative models on time-scales relevant in this work in few analyses of the LC patterns (Alvera-Azcárate et al., 2009; Liu et al., 2011; 2016; Weisberg and Liu, 2017). The GCOOS SSH product is obtained by applying objective mapping to along-track satellite altimetry, then gridding the outcome on a $0.25^{\circ} \times 0.25^{\circ}$ latitude-longitude grid with daily sampling. As a result, the effective spatiotemporal resolution of the gridded product is lower than its nominal one (see e.g. Ballarotta et al., 2019 for a general discussion of this problem) and of HYCOM. Given the size of the mesoscale structures in the GoM, and the fact that the attractor describes the larger, dominant dynamics, the spatial resolution remains sufficient to resolve the attractor's dimension. In terms of temporal resolution, on the other hand, the orbital characteristics and repeat cycles of altimeters, that in the GoM vary between 10 and 35 days depending on the satellite, may suppress temporal variations up to $\sim$ 10-14 days (Ballarotta et al., 2019). To account for it, we low-passed GCOOS and Hycom data using Butterworth filter with a 14-days cutoff frequency.

3 Results

A key characteristic in the evolution of the LC is its penetration into the northern Gulf of Mexico and the apparent stability in its extended configuration lasting up to several months, which is seldom captured by forecasting models (NASEM, 2018). Figure 1 shows an example of this state, dating to July 2011. In the reanalysis the LC appears closer to separating an eddy than in the observations despite the assimilation of sea surface height data. The domain used in this investigation is also indicated in Figure 1. We separately considered a domain to the west of it with identical size, where the Rings are the most prominent mesoscale pattern. A number of degrees of freedom larger than that for the LC is expected to describe the Rings' trajectory across the Gulf, being eddiesless recurrent and more chaotic, and this is verified in the Suppl. Information (SI).

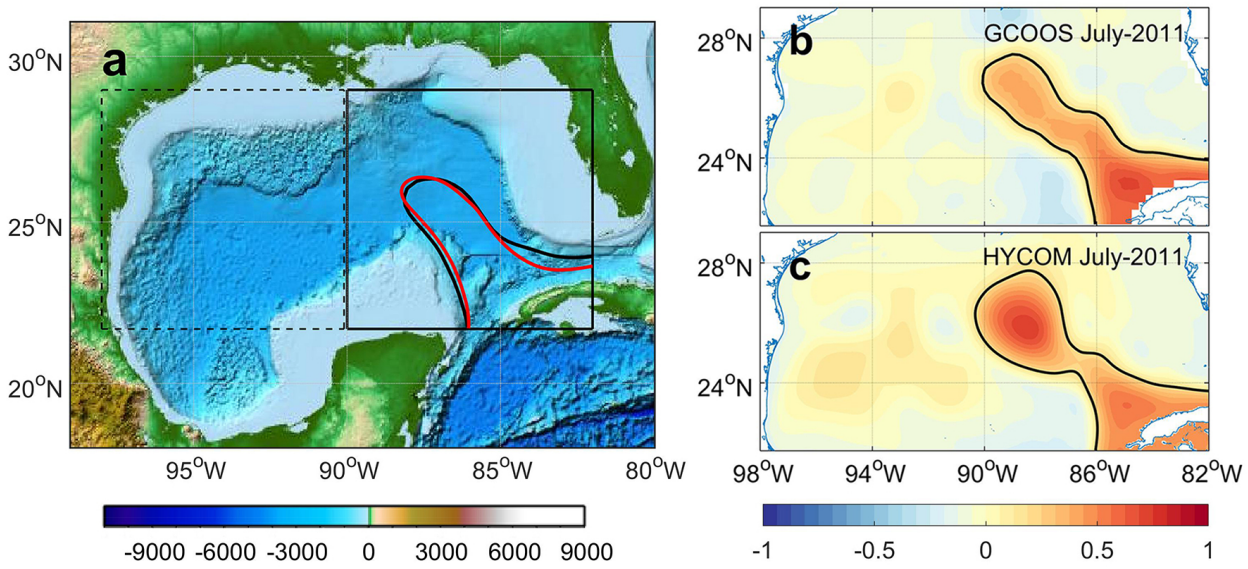

Figure 1. a) Domain considered in our analysis indicated by the black box with the mean 0.2 m sea surface height anomaly contour averaged over the period of 01/2004 to 12/2012 normalized to have zero-mean. Color shading represents bathymetry, GCOOS is indicated in black and HYCOM in red. The analysis over the western domain (dashed black box) is presented in the SI. b) and c) SSHa normalized to have zero mean and averaged over the month of July 2011 in GCOOS and HYCOM; Units: m.

Figure 2 visualizes the LC attractor as a 3-dimensional phase space projection of the first three principal components, PC1, PC2 and PC3 over the sixteen years considered in GCOOS and Hycom. The low-dimensional projection highlights qualitatively different dynamics among datasets, with somewhat *straighter* trajectories in the altimeter dataset and a rotation difference of about 30° - 40°. The first principal components are well correlated, with a Pearson coefficient of 0.87, but the correlation decreases to 0.59 for PC2 and 0.57 for PC3. The PCs explain respectively 23%, 21% and 15% of the variance in GCOOS and similarly 25%, 21% and 13% in Hycom. The correlations and the variance explained do not depend on the filtering and we verified that analogous values are found using daily unfiltered data or 10-days low-pass filtered data. High values of PC2 correspond to LC shedding events or shedding and re-attaching events, which tend to be slightly overestimated by Hycom compared to GCOOS. This can be seen in the video of the time evolution of PC2 and SSHa available in the Suppl. Information; large differences in the two datasets are found, for example, around July 14$^{\text{th}}$, 2005, October 25$^{\text{th}}$, 2007, July 2011, September – October 2014.

The instantaneous dimension time-series for the two datasets are shown in Figure 3, together with their probability density function and a zoom of the attrac-

tor manifolds over 2009-2016 colored by their respective d values. This shorter period covers the Deepwater Horizon (DHW) disaster, when despite many in-situ observations being collected most forecast models predicted the spinoff of a Ring in spring, which did not occur until well into the summer, and a prolonged time between the second half of 2014 and spring of 2015 during which the LC was in an extended state but stable, and its forecast was poor. Also in this occasion, model forecasts continued to predict shedding events, while the LC remained in an extended state most of the time. In both cases the PC1 evolution is captured by Hycom, but PC2 differs significantly among datasets.

Several features further emerge from Figure 3. First, the average dimension D of the LC is around 9.5 in both datasets, or in other words, less than 10 DoF are on average sufficient to describe its dynamics. Its distribution is overall well captured by Hycom even if underestimated in its right tail (it is worth noting that in the western domain Hycom underestimates more significantly GCOOS $d(\ )$, as shown in the SI). Twenty or more DoF, however, are needed whenever the LC transitions from an elongated to a retracted state and immediately following Ring shedding events (see the video in the SI). This analysis indicates that low-dimensional models cannot capture the complexity of the LC transitions and the shedding of the Rings. We verified that the averaged dimension is insensitive to the low-pass filtering.

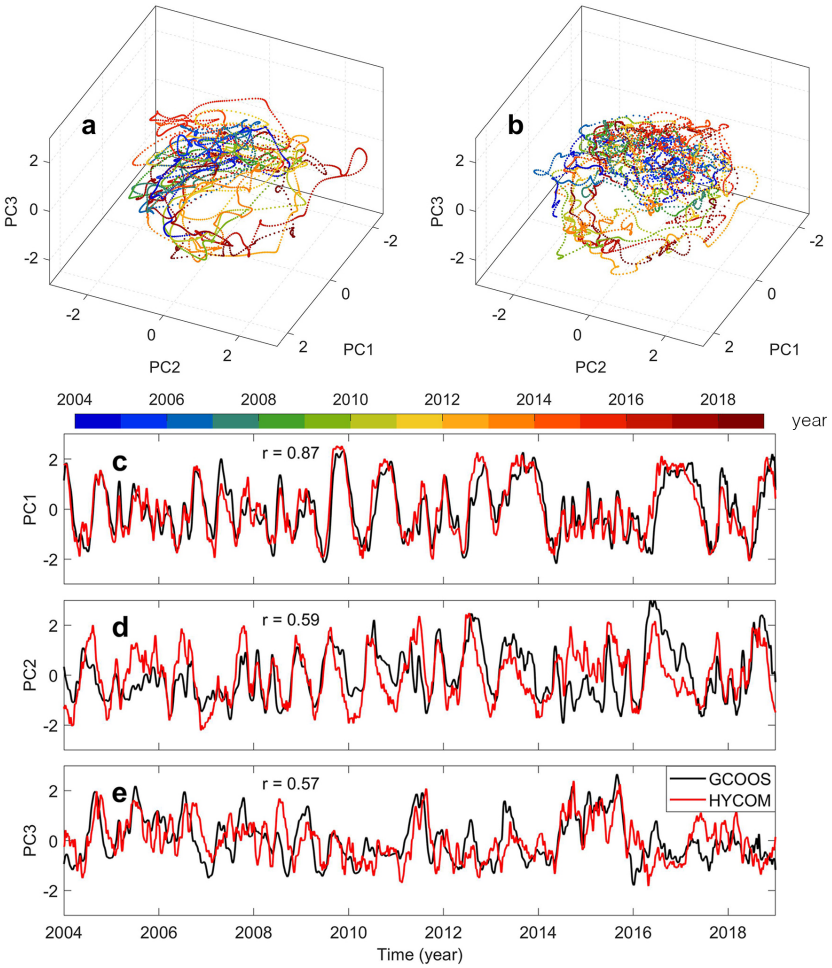

Figure 2. LC attractor shown as a 3-dimensional phase space projection of the first three principal components in (a) GCOOS and (b) Hycom. (c) PC1, (d) PC2 and (e) PC3 time series for the two datasets.

The correlation coefficient between d time-series in GCOOS and Hycom is only 0.35. Large discrepancies can point to forecasting issues. For example, in spring and summer of 2010, during the DWH spill, the LC was in an extended state in April and retreated at the end of the month, until May. An anticyclonic eddy began forming towards the end of May 2010, but the LC remained fairly to the south (Liu et al., 2011), contributing with its state to maintaining the surface oil sleek in the northeastern Gulf and away from Florida. Forecasting was problematic, and an overestimation of the instantaneous dimension in May is apparent in the reanalysis (Figure 3a).

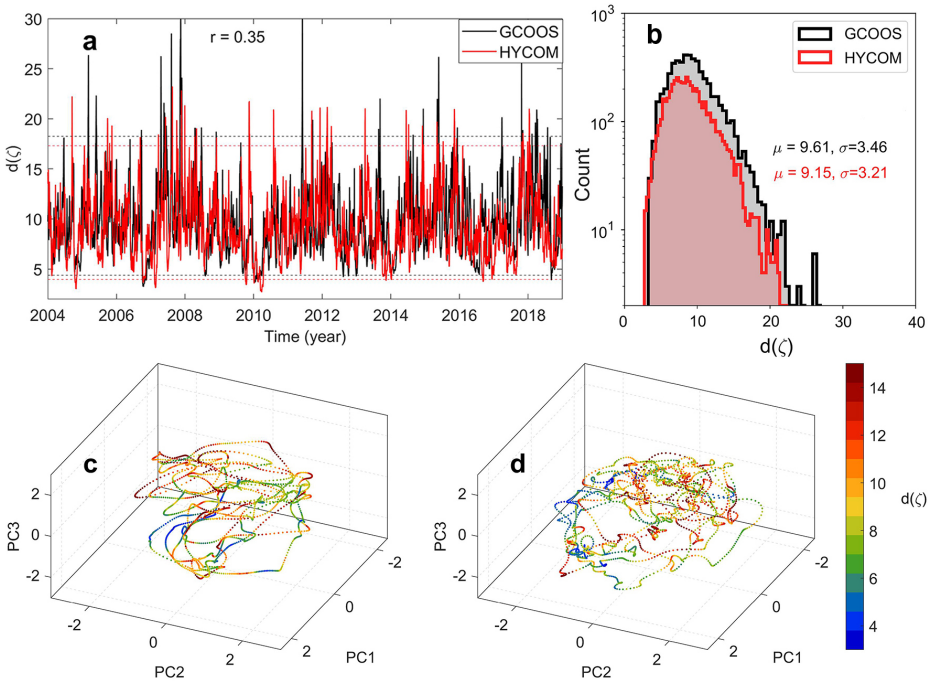

Figure 3. (a) Daily time evolution of $d(\,)$ based on low-pass filtered data. Horizontal dotted lines indicate the 2^{nd} and 98^{th} percentiles for GCOOS (black) and Hycom (red) below and above which the LC state is presented in Figure 4. (b) Probability density functions (PDFs) of $d(\,)$ in GCOOS and Hycom. (c) and (d) Attractors colored by d values over the 2009-2016 period in GCOOS and Hycom, respectively.

It is worth remarking that the dynamics described by the attractor with dimension D is that of the large mesoscale features and is essentially unaffected by small scale circulations. As such, the evolution of d in Hycom is nearly identical if the model output is upscaled to the (spatial) resolution of GCOOS. This has been verified by spatially interpolating or downsampling Hycom data to GCOOS resolution or by applying a six-by-six grid point low-pass filter to Hycom that acts to remove information on dynamical processes at smaller scales (not shown).

Finally, Figure 4 exemplifies typical configurations that require far below average ($< 2^{\text{nd}}$ percentile) and above average ($> 98^{\text{th}}$ percentile) degrees of freedom for their description according to Figure 3. Retracted LC configurations (Figure 4a-b) are responsible for the minima. Noticeably two recurrent quasi-stable states can be identified, with the LC extending to $\sim 25.5^{\text{o}}$N or just above 26^{o}N. These two states are closer in GCOOS and better separated in Hycom. For the relative maxima in d, on the other hand, the LC is found most frequently in its extended stage immediately before and after a LCE detachment, and more recurrent or preferred LC trajectories can be identified in GCOOS compared to

Hycom.

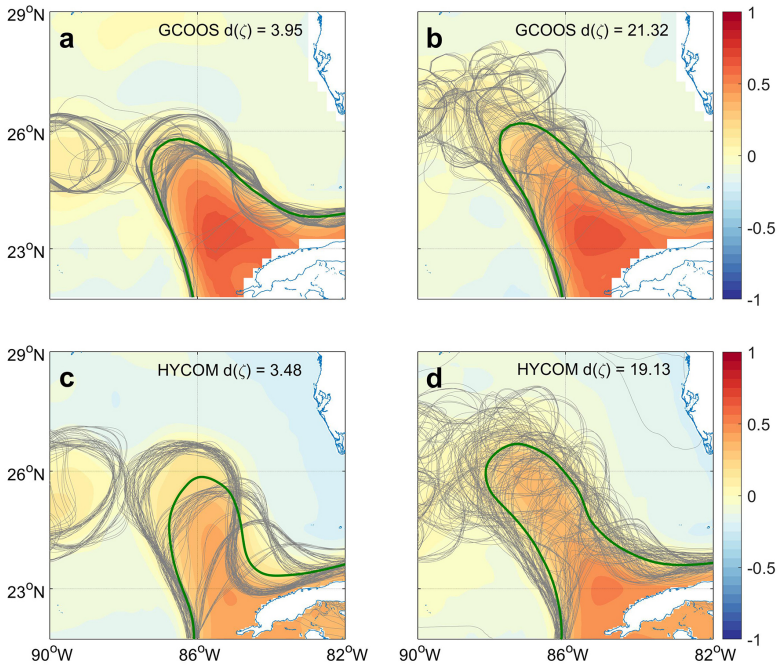

Figure 4. GCOOS and Hycom SSHa patterns normalized to zero-mean for episodes of low $d(\ )$ (below 2$^{\text{nd}}$ percentile, a and c) and large $d(\ )$ (above 98$^{\text{th}}$ percentile, c and d). Green contours indicate the 0.2 m contour in the mean SSHa field. Thin gray contours indicate the 0.2 m SSHa contour of each event in the two groups; $d(\ )$ average values for each case are indicated in the legends.

4 Discussion and Conclusions

We characterized the Loop Current attractor via a novel dynamical system metric and compared it in altimeter-derived SSH data and in HYCOM products over 16 years. The instantaneous dimension d is linked to predictability, with states characterized by low d values being more predictable and vice versa (Faranda et al., 2017). The LC has a relatively low instantaneous dimension and less than 10 DoF are sufficient to describe the average dimension of its attractor, with a few episodes that deviate strongly, whenever a Ring is formed and detaches from the current. Our comparison supports the notion that the LC phase-space trajectory is more stable in GCOOS than in simulated data-assimilative products given the characteristics of the attractor trajectories. This is in agreement with recent theoretical results (Sheremet et al., 2021) and with the widespread conjecture that forecast skills could be improved in forecast models (NASEM, 2018).

The simultaneous evaluation of d and of the first three principal components on which the n-dimensional attractor manifold has been projected, allows us to dis-

tinguish between extended LC events that last several months and those that result in the shedding of a Ring, and can inform operational ocean forecasts. It is conventional wisdom that forecast models and ocean models in general tend to overestimate the rate of formation of Rings in the Gulf of Mexico, with poignant examples in spring 2010 and in fall 2014 into spring 2015 (see NASEM 2018 for an in-depth discussion of the limitations in ocean forecasts for the LC system). Among the causes for the discrepancy, a lack of mesoscale air–sea interaction with the atmosphere in ocean-only model runs could concentrate too much energy in the mesoscale structures and increase the instability potential of the LC, similarly to what was found for western boundary currents (Ma et al., 2016; Renault et al., 2016). Alternatively, current ocean models may be unable to correctly represent processes inherently related to the stability properties of the attractor, as for example diffusive processes, and may not capture properly the steady states of the system (Pichevin and Nof, 1997; Kuehl and Sheremet, 2014). This last possibility has been recently suggested by Sheremet et al. (2021).

In summary, our work introduces to the ocean community a tool for quantifying model biases that opens new pathways for improving forecast skill. For example, short-term forecasts improvements could be achieved by coupling existing data-assimilative models with machine-learning data-driven techniques to constrain the LC spatiotemporal dynamics to the observed attractor dimensionality. Alternatively, for forecasts on times longer than 2 - 3 weeks manifold learning methodologies could prove useful. A growing subfield of machine learning, manifold learning builds upon the assumption that observed data lie on a low-dimensional manifold embedded in a higher-dimensional space: in the LC case nearly 60% of the variance is captured by the first 3 principal components and d is usually less than 20. The adoption of nonlinear algorithms instead of linear PC analysis for dimensional reduction may further improve the amount of variance captured by the first few components (Falasca and Bracco, 2021). Predicting the evolution of these few components could prove easier than forecasting the evolution of the physical system. Furthermore, a simplified but physically-based model coupled with manifold learning could facilitate the prediction of specific events, such as the shedding of a Ring or an enduring extended state.

To conclude, the above suggested strategies for improving forecast and simulations of the Loop Current behavior, may not extend to a generic ocean system, as they build upon the concept of recurrence (Lucarini et al., 2016). In the Supplementary Information we show that forecasting the movement of the Rings or large eddies in general poses a greater challenge, with d being larger, the disagreement among principal components in GCOOS and Hycom much higher, and most importantly the variance explained by the first three PCs small. The LC has been shown to behave as a nonlinear, dampened oscillator (Lugo-Fernández, 2007), while eddies are intrinsically chaotic.

Acknowledgments

This work was supported by the Gulf Research Program (GRP) of the Na-

tional Academies of Sciences, Engineering, and Medicine through its Understanding Gulf Ocean Systems 2 (UGOS-2) Grant "The Loop Current and the Mississippi-Atchafalaya River System: Interactions, Variability and Modeling Requirements" (GL and AB) and by the Department of Energy, Regional and Global Model Analysis (RGMA) Program, Grant Number: 0000253789. We thank J. Kuehl who motivated this analysis through his recent results.

Data Availability

All datasets analyzed in this work are publicly available. The GCOOS seas surface height data can be downloaded at https://geo.gcoos.org/ssh/ (last access: 08/17/2021). The HYCOM sea surface height data can be accessed through the https://www.hycom.org/dataserver (https://www.hycom.org/data/gomu0pt04/expt-50pt1, https://www.hycom.org/data/goml0pt04/expt-31pt0, and https://www.hycom.org/data/goml0pt04/expt-32pt5) (last access: 08/17/2021).

The python codes for the metrics applied can be found at https://github.com/yrobink/CDSK/tree/master/python/CDSK and will be deposited in a permanent archive such as Zenodo upon revision/acceptance.

References

Alvera-Azcárate, A., Barth A., & Weisberg, R. H. (2009). The surface circulation of the Caribbean Sea and the Gulf of Mexico as inferred from satellite altimetry. *Journal of Physical Oceanography*, *39*(3), 640-657, doi:10.1175/2008JPO3765.1.

Ballarotta, M., Ubelmann, C., Pujol, M. –I., & Taburet, G. et al. (2019). On the resolutions of ocean altimetry maps. *Ocean Science*, *15*(4), 1091-1109, doi:10.5194/os-15-1091-2019.

Cummings, J., & Smedstad, O. (2013). Variational data assimilation for the global ocean. *Data Assimilation for Atmospheric, Oceanic and Hydrologic Applications*, *2*, 303-343, doi:10.1007/978-3-642-35088-7_13.

De Luca, P., Messori, G., Pons, F.M.E. & Faranda, D. (2020) Dynamical systems theory sheds new light on compound climate extremes in Europe and Eastern North America. *Quart. J. Royal Meteorol Soc.*, 146:1636–1650, https://doi.org/10.1002/qj.3757

Dijkstra, H. A. (2000) *Nonlinear Physical Oceanography*, Kluwer Academic Publishers, Dordrecht, The Netherlands.

Falasca, F. and Bracco, F. (2021). Exploring the climate system through manifold learning. arXiv:2110.03614

Faranda, D., Alvarez-Castro, M. C., & Yiou, P. (2016). Return times of hot and cold days via recurrences and extreme value theory. *Climate Dynamics*, *47*(12), 3803-3815, doi:10.1007/s00382-016-3042-6.

Faranda, D., Messori, G., & Yiou, P. (2017). Dynamical proxies of North Atlantic predictability and extremes. *Scientific Report*, *7*, 41278, doi:10.1038/srep41278.

Freitas, A. C. M., Freitas, J. M. & Todd, M (2010). Hitting time statistics and extreme value theory. *Probability Theory and Related Fields*, 147:675–710.

Foias, C., Sell, G. R., and Témam, R. (1988), Inertial manifolds for nonlinear evolu-
tionary equations, J. Diff. Equ., vol. 73, pp. 309–353

Gopalakrishnan, G., Cornuelle, B. D., & Hoteit, I. (2013). Adjoint sensitivity studies of loop current and eddy shedding in the Gulf of Mexico. *Journal of Geophysical Research: Oceans*, *118*(7), 3315-3335, doi:10.1002/jgrc.20240.

Gordon, A. L. (1967). Circulation of the Caribbean Sea. *Journal of Geophysical Research*, *72*, 6207, doi:10.1029/JZ072i024p06207.

Gudorf, M.N. (2020), Spatiotemporal tiling of the Kuramoto-Sivashinky equation. PhD Thesis, Georgia Tech Library http://hdl.handle.net/1853/64158

Hall, C. A., & Leben, R. R. (2016). Observational evidence of seasonality in the timing of loop current eddy separation. *Dynamics of Atmospheres and Oceans*, *76*, 240-267, doi:10.1016/j.dynatmoce.2016.06.002.

Hamilton, P. (1990). Deep currents in the Gulf of Mexico, *Journal of Physical Oceanography, 20*(7), 1087-1104, https://doi.org/10.1175/1520-0485(1990)020<1087:DCITGO>2.0.CO;2

Hochman, A., Alpert, P., Harpaz, T., Saaroni, H. & Messori, G. (2019). A new dynamical systems perspective on atmospheric predictability: Eastern Mediterranean weather regimes as a case study. *Science Adv.,* 5(6), eaau0936, doi: 10.1126/sciadv.aau0936

Johns, W. E., Townsend, T. L., Fratantoni, D. M., & Wilson, W. D. (2002). On the Atlantic inflow to the Caribbean Sea. *Deep Sea Research Part I: Oceanographic Research Papers*, *49*(2), 211-243, doi:https://doi.org/10.1016/S0967-0637(01)00041-3.

Kuehl, J. J., Sheremet, V. A. (2014) Two-layer gap-leaping oceanic boundary currents: experimental investigation. *J. Fluid Mech.* 740, 97-113. doi:10.1017/jfm.2013.645

Leadbetter, M.R. (1983). Extremes and local dependence in stationary sequences. *Wahrscheinlichkeitstheorie verw Gebiete* 65, 291–306. https://doi.org/10.1007/BF00532484

Leben, R.R., Born, G.H., Engelbrecht, B.R. (2002). Operational altimeter data processing for mesoscale monitoring, *Marine Geodesy*, 25:3-18.

Lipphardt„ B. L., Poje, A. C., Kirwan, A. D., Kantha, L., Zweng, M. (2008) Death of three Loop Current rings. *J. Marine Research*, 66, 25-60,

https://doi.org/10.1357/002224008784815748

Liu, Y., MacFadyen, A., Ji, Z.-G., & Weisberg, R. H. (2011). Monitoring and modeling the Deepwater Horizon oil spill: A record-breaking enterprise. *Washington DC American Geophysical Union Geophysical Monograph Series*, *195*, doi:10.1029/gm195.

Liu, Y., Weisberg, R. H., Vignudelli, S., & Mitchum, G. T. (2014). Evaluation of altimetry-derived surface current products using Lagrangian drifter trajectories in the eastern Gulf of Mexico. *Journal of Geophysical Research: Oceans*, *119*(5), 2827-2842, doi:10.1002/2013jc009710.

Liu, Y., Weisberg, R. H., Vignudelli, S., & Mitchum, G. T., (2016). Patterns of the loop current system and regions of sea surface height variability in the eastern Gulf of Mexico revealed by the self-organizing maps. *Journal of Geophysical Research: Oceans*, *121*(4), 2347-2366, doi:10.1002/2015jc011493.

Lorenz, E. N. (1980). Attractor sets and Quasi-Geostrophic equilibrium. *Journal of Atmospheric Sciences*, *37*(8), 1685-1699, doi:10.1175/1520-0469(1980)037<1685:ASAQGE>2.0.CO;2.

Lucarini, V., Faranda, D., de Freitas, J. M. M., & Holland, M., et al. (2016). *Extremes and recurrence in dynamical systems*. John Wiley & Sons.

Lugo-Fernández, A. (2007). Is the Loop Current a Chaotic Oscillator? *Journal of Physical Oceanography*, 37, 1455-1469, doi: 10.1175/JPO3066.1

Ma, X., Jing, Z., Chang, P., & Liu, X. et al. (2016). Western boundary currents regulated by interaction between ocean eddies and the atmosphere. *Nature*, *535*(7613), 533-537, doi:10.1038/nature18640.

McMahon, C. W., Kuehl, J. J., & Sheremet, V. A. (2021). Dynamics of gap-leaping western boundary currents with throughflow forcing. *Journal of Physical Oceanography*, doi:10.1175/jpo-d-20-0216.1.

Messori, G., Harnik, N., Madonna, E., & Lachmy, O. et al. (2021). A dynamical systems characterization of atmospheric jet regimes. *Earth System Dynamics*, *12*(1), 233-251, doi:10.5194/esd-12-233-2021.

NASEM (National Academies of Sciences, Engineering and Medicine) (2018). *Understanding and Predicting the Gulf of Mexico Loop Current: Critical Gaps and Recommendations*, 116 pp., The National Academies Press, Washington, DC, doi:doi:10.17226/24823.

Pichevin, T., Nof, D. (1997) The momentum imbalance paradox. *Tellus*, 49, 298-319, https://doi.org/10.3402/tellusa.v49i2.14484

Primeau, F. W. (1998). Multiple equilibria of a double-gyre ocean model with super-slip boundary conditions. *Journal of Physical Oceanography*, *28*(11), 2130-2147, doi:10.1175/1520-0485(1998)028<2130:MEOADG>2.0.CO;2.

Renault, L., Molemaker, M. J., McWilliams, J. C., & Shchepetkin, A. F. et al. (2016). Modulation of wind work by oceanic current interaction with the atmosphere. *Journal of Physical Oceanography*, *46*(6), 1685-1704, doi:10.1175/jpo-d-15-0232.1.

Saha, S., Moorthi, S., Pan, H. –L., & Wu, X. et al. (2010). The NCEP climate forecast system reanalysis. *Bulletin of the American Meteorological Society*, *91*(8), 1015-1058, doi:10.1175/2010BAMS3001.1.

Sheremet, V. A., Khan, A. A., & Kuehl, J. J. (2021). Multiple equilibrium states of the Loop Current in the Gulf of Mexico. *Journal of Physical Oceanography*, submitted.

Vautard, R., & Ghil, M. (1989). Singular spectrum analysis in nonlinear dynamics, with applications to paleoclimatic time series. *Physica D: Nonlinear Phenomena*, *35*(3), 395-424, doi:https://doi.org/10.1016/0167-2789(89)90077-8.

Weisberg, R. H., & Liu, Y. (2017). On the Loop Current penetration into the Gulf of Mexico. *Journal of Geophysical Research: Oceans*, *122*(12), 9679-9694, doi:10.1002/2017jc013330.